Optimization of rutin encapsulation in self-assembled polymeric particles

Narinchote Kaiyoonwong[1], Natthaporn Sae-lim[2] and Kamolchanok Ngamkham[2,*]

[1]The Biopharmaceutical Engineering Practice School, Department of Chemical Engineering, Faculty of Engineering, King Mongkutt's University of Technology Thonburi, Bangkok, 10140, Thailand.

[2]Biological Engineering Program, Faculty of Engineering, King Mongkutt's University of Technology Thonburi, Bangkok, 10140, Thailand.

Abstract.

Rutin is a polyphenolic compound found in several fruits and vegetables. It possesses various therapeutic properties, including antioxidant, anti-inflammatory, anti-cancer, and anti-microbial. Moreover, rutin was also reported to enhance stem cell proliferation and differentiation. However, the applications of rutin are limited as it has low water solubility and low bioavailability. To overcome those limitations, in this study, rutin was encapsulated with a self-assembled amphiphilic block copolymer, poly(lactide)-b-poly(poly ethylene glycol methacrylate) (PLA-b-PPEGMA), using the solvent switch method. Different amounts of rutin and water volume have been tried and the highest encapsulation efficiency was achieved when 10 mg block copolymer was used to encapsulate 0.5 mg rutin in 5 ml water at the polymer dropping rate of 300 µl/min. The encapsulation efficiency is up to 35.04 ± 3.52 wt% and a drug loading capacity is 1.75 ± 0.176 wt% with an average particle size of 1.90 ± 0.71 µm. Nevertheless, the encapsulation efficiency and drug loading capacity can be improved by lowering the polymer dropping rate. The best condition was presented on 100 µl/min dropping rate which exhibited 65.32 ± 11.69% encapsulation and 3.27 ± 0.58% drug loading capacity, respectively. Moreover, the release of rutin from the particles was sustained for more than 4 hours, while free rutin reached 100% released after 45 minutes. The release mechanism was most fitted to the Weibull model with a shape parameter indicating a complex release mechanism. This research optimized a drug encapsulation protocol for making a micro-scale rutin delivery carrier which can be utilized with further drug delivery applications.

Keywords: diblock copolymer; drug release; particles; rutin encapsulation; self-assembly

1. Introduction

Rutin, a quercetin glycoside or vitamin P, is a flavonol compound found in many plants such as buckwheat, caper bush, passionflower, and apple (Ganeshpurkar & Saluja, 2017; Kianersi et al., 2020). It displays pharmacological actions in various systems of the human body as it possesses antioxidant, anti-inflammatory, anticarcinogenic, antithrombotic, antimicrobial,

neuroprotective, and cardioprotective properties (Ganeshpurkar & Saluja, 2017; Su et al., 2014). Even though the therapeutic potentials of rutin are diverse, its applications are limited due to its poor aqueous solubility and low bioavailability. Thus, many researchers are trying to overcome these limitations to reach the full benefit of this natural compound.

Encapsulation is one of the frequently used strategies in drug delivery systems as it can cope with some conventional limitations and improve the effectiveness of treatment. The drugs or active agents could be protected, solubility could be enhanced and the sustained or controlled release could be archived via encapsulation (Martínez Rivas et al., 2017). Various encapsulation methods and materials have been developed and utilized for different purposes (Martínez Rivas et al., 2017; Trucillo, 2021). Amphiphilic block copolymers which comprise two or more immiscible blocks are among the extensively studied materials for drug encapsulation. Due to the ability to self-assemble in an aqueous solution, different structures could be simply formed by amphiphilic block copolymers (Avsar et al., 2019; Cabral et al., 2018).

For *in vivo* applications, the safety of block copolymer utilized in drug encapsulation is needed to be concerned. Biocompatible and biodegradable polymers are preferred in this approach. Poly(lactide)-b-poly(polyethylene glycol methacrylate) (PLA-b-PPEGMA) is an amphiphilic block copolymer that meets this criteria. PLA, a hydrophobic polyester, has long been used as a biomedical material and got approved by Food and Drug Administration (FDA) for clinical use (Casalini et al., 2019). While PPEGMA is a hydrophilic polymer with protein resistance and low antigenicity properties (Joh et al., 2019). Thus, particles forming by a copolymer of PLA and PPEGMA would be suitable as a drug carrier since they combine the characteristic properties of both polymers.

In this research, encapsulation of rutin by PLA-PPEGMA amphiphilic block polymer using solvent switch method was optimized. Parameters involved in drug encapsulation such as water volume, amount of drug used, and polymer dropping rates were varied. Encapsulation efficiency, drug loading capacity, size, and morphology of rutin-encapsulated PLA-PPEGMA particles were evaluated. *In vitro* rutin release from the particles and a suitable drug release model were also determined.

2. Materials and Methods

2.1 Materials

The poly(ethylene glycol) methacrylate (hydroxyl-terminated) (M_n 500), Poly(L-lactide) 4-cyano-4-[(dodecylsulfanylthiocarbonyl)sulfanyl]pentonate (PLA-CTA), 1,2-dichloroethane (anhydrous), and azobisisobutyronitrile (AIBN) were obtained from Sigma Aldrich. Methanol, chloroform, and acetone were purchased from RCI Labscan. Rutin hydrate was received from Tokyo Chemical Industry. Regenerated cellulose membrane with molecular weight cut-off (MWCO) of 12,000 – 14,000 Da was obtained from MFPI.

2.2 Synthesis of PLA-PPEGMA block copolymer

PEGMA (1820 µL, 4 mmol), PLA-CTA (0.5 g, 0.5mmol) and AIBN (180 µL, 0.036mmol) were mixed with 24 mL dichloroethane in 25 mL round bottom flask under stirring condition.

The flask was sealed with a rubber septum and the mixture was deoxygenated with N_2 gas for 20 min. The reaction was then carried at 75 °C in an oil bath for 24 h. To stop the polymerization, the resulting solution was cooled to 20 °C and transferred to the dialysis membrane. The dialysis was carried against acetone for 3 days. The purified block copolymers were then dried in a vacuum desiccator. PLA-PPEGMA obtained was characterized using ^1H NMR in $CDCl_3$ at room temperature (Bruker NMR spectrometer, 400 MHz) and GPC analysis with Waters 2414 refractive index (RI) detector, geared up with Styragel HR5E 7.8 × 300 mm column. The columns were eluted using tetrahydrofuran with a flow rate of 1.0 mL/min at 40 °C and calibrated with polystyrene standard.

2.3 Formation of rutin-loaded PLA-PPEGMA particles

Self-assembled nanoparticles were formed using the solvent switch method. To observe the suitable condition for rutin encapsulation, 10 mg of PLA-PPEGMA was dissolved in chloroform and various amount of stock rutin (5 mg/ml in methanol) was mixed with a polymer solution as shown in table 1. The mixture was then added drop-wise to 5 or 10 mL of stirring distilled water at the dropping rate of approximately 300 µl/min. The solvent was removed by stirring for another 2 h. The particles were separated from free rutin using centrifugation technique (20 min, 12,500 rpm, 4 °C) and washed again with distilled water to get rid of the unbounded and loosely associated rutin. Another round of centrifugation was performed, and the particles collected were resuspended in 1 mL of distilled water. The effects of different polymer dropping rates (100, 200 and 300 µl/min) were also evaluated.

Table 1: Encapsulation conditions

Condition	Polymer)mg(	Water)mL(	Rutin)mg(
1	10	5	0.5
2	10	5	0.75
3	10	5	1.0
4	10	10	0.5
5	10	10	0.75
6	10	10	1.0

2.4 Quantification of encapsulation efficiency and drug loading capacity

Rutin amount that remained in the supernatant of the encapsulated particles was determined using spectrophotometry. The absorbance of the supernatant at 360 nm was compared to the rutin standard. The encapsulation efficiency and drug loading capacity can be calculated by equations (1) and (2):

$$\text{Encapsulation Efficiency} = \left(\frac{\text{Mass of drug encapsulated}}{\text{Mass of initial drug feed}}\right) \text{x } 100 \quad (1)$$

$$\text{Drug Loading Capacity} = \left(\frac{\text{Mass of drug encapsulated}}{\text{Mass of the polymer}}\right) \text{x } 100 \quad (2)$$

2.5 Visualization of rutin-loaded PLA-PPEGMA particles

The morphology of encapsulated particles was analyzed using the scanning electron microscope (SEM), JEOL JSM-6610LV series. The samples were dried using a vacuum oven at the temperature of 35 °C and attached to the stubs with carbon tape. The samples were sputter

coating with gold and the SEM was operated at the voltages of 10 kV. The particle size was determined from the provided scale bar in SEM images using Image J software.

2.5 Determination of *in vitro* rutin release profile

The particles were resuspended in 3 ml phosphate buffer saline (PBS), and then transfer into dialysis membrane MWCO 12-14 kDa against 10 ml PBS in a 50 ml tube which was incubated in a 37 °C shaking incubator with an agitation speed of 300 rpm. 10 ml of each sample was collected at 5, 10, 15, 30, 45 min, 1 hr, 1.5 hr, 2 hr, 2.5 hr, 3 hr, and 4 hr to determine the cumulative released percentage by UV-spectroscopy against the standard curve. Moreover, the experimental data was plotted with KinetDS software to determine the possible release mechanism.

3. Results and Discussion

3.1 Synthesis and characterization of PLA-PPEGMA block copolymer

PLA-PPEGMA was synthesized by reversible addition fragmentation chain-transfer polymerization (RAFT) and characterized by ^{1}H NMR. All the characteristic peaks of the molecules were presented as shown in Figure 1A and coincide with the previous study of a similar polymer (Themistou et al., 2014). The slight difference is that the end group of our PPEGMA is a hydroxyl instead of a methyl group. The molecular weight of the polymer was also determined by GPC. The Mw of 41541g/mol and the Mn of 26099 g/mol PLA-PPEGMA copolymer was obtained (Figure 1B). This block copolymer indicated a relatively broad PDI (Mw/Mn) of 1.59.

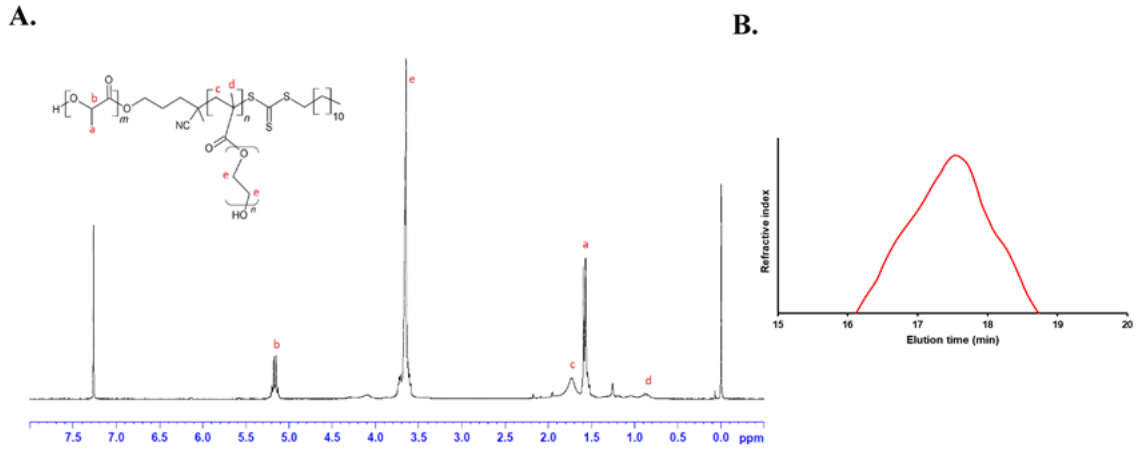

Figure 1: PLA-PPEGMA characterization. A) ^{1}H NMR Spectra and B) GPC curve of the obtained PLA-PPEGMA block copolymer.

3.2 Encapsulation efficiency and drug loading capacity of rutin-loaded PLA-PPEGMA particles

The encapsulation of 0.5 mg, 0.75 mg, and 1 mg rutin amount under 2 different water volumes, 5 and 10 mL, have been investigated. The PLA-PPEGMA used to encapsulate the rutin was fixed at 10 mg and the polymer dropping rate was fixed at 300 µl/min. To investigate the

encapsulation efficiency and drug loading capacity, the absorbance of the standards and supernatants were analyzed by the UV-spectrophotometric method at 360 nm. The concentration and amount of rutin in the supernatant after encapsulation were calculated from the standard curve.

From Table 2, the encapsulation efficiency of 0.5 mg, 0.75 mg and 1 mg rutin under 5 mL water volume were 35.04 ± 3.52%, 26.35 ± 5.50% and 22.16 ± 0.77% respectively. The encapsulation efficiencies tend to decrease according to the increase in rutin amount. The reason is due to the limitation of 10 mg PLA-PPEGMA encapsulation ability. Furthermore, the drug loading capacity in this case were 1.75 ± 0.176%, 1.97 ± 0.412% and 2.21 ± 0.077% subsequently.

In the aspect of rutin encapsulation by PLA-PPEGMA under 10 mL water volume, the operation was done similarly to the previous protocol. The encapsulation efficiencies of this condition under the same variation of rutin amounts were 26.16 ± 1.45%, 18.04 ± 0.86%, and 10.43 ± 0.75% accordingly. Similar to the earlier condition, the trend of encapsulation efficiency was inversely proportional to the rutin amount. Additionally, the drug loading capacity of 0.5 mg, 0.75 mg and 1 mg rutin amount were 1.31 ± 0.072%, 1.35 ± 0.065%, and 1.04 ± 0.075% respectively. According to table 2, the encapsulation efficiency and drug loading capacity of rutin encapsulation protocol under 5 mL water were more than that of 10 mL water in all cases.

Compared to the previous work, which tried to encapsulate the hydrophobic drug using PLGA-PEG by precipitation technique, the encapsulation efficiencies of our work are significantly higher (Xu et al., 2019). Thus, this result ensured the ability of rutin encapsulation by PLA-PPEGMA under the solvent switch method. However, compared to the work of Kizilbey et al., that encapsulated rutin using oil in water single emulsion solvent evaporation method, the encapsulation efficiency under the same polymer to drug proportion of our work is still lower (Kizilbey, 2019). However, we can still improve the encapsulation efficiency by simply reducing the flow rate of dropping polymer as previously reported (Fund et al., 2018; Motlekar, 2009).

In summary, for all rutin amounts, the encapsulation efficiency and drug loading capacity are higher in the experiment with 5 mL water volume. Since there is no significant difference in drug loading capacity, the best encapsulation case belongs to 0.5 mg rutin encapsulated by 10 mg PLA-PPEGMA under 5 mL water volume with the highest encapsulation efficiency of 35.04 ± 3.52%.

Table 2: Effects of parameters on encapsulation efficiency and drug loading capacity.

Condition	Polymer)mg(	Water)mL(	Rutin)mg(	Encapsulation Efficiency (%)	Drug loading capacity (%)
1	10	5	0.5	35.04 ± 3.52	1.75 ± 0.176
2	10	5	0.75	26.35 ±5.50	1.97 ± 0.412
3	10	5	1.0	22.16 ± 0.77	2.21 ± 0.077
4	10	10	0.5	26.16 ± 1.45	1.31 ± 0.072
5	10	10	0.75	18.04 ± 0.86	1.35 ± 0.065
6	10	10	1.0	10.43 ± 0.75	1.04 ± 0.075

To improve the encapsulation efficiency and drug loading capacity, different polymer dropping rate including 100, 200, and 300 µl/min were tried. Higher encapsulation efficiency and drug loading capacity were observed when the polymer dropping rate decreased. The encapsulation efficiency of 100, 200 and 300 µl/min dropping rates were 65.32 ± 11.69%, 48.14 ± 1.82% and 35.04 ± 3.53% respectively (Figure 2A). A significant difference was detected between 100 and 300 µl/min conditions ($p<0.01$). The results for drug loading capacity also showed a similar trend. The lowest drug loading capacity was observed in 300 µl/min condition while increasing percentages were detected on 100 and 200 µl/min conditions with the value of 3.27 ± 0.58% and 2.41 ± 0.09% respectively (Figure 2B). A significant difference was also detected between 100 and 300 µl/min conditions ($p<0.01$). So, to achieve the highest rutin encapsulation efficiency, a slow polymer dropping rate is needed.

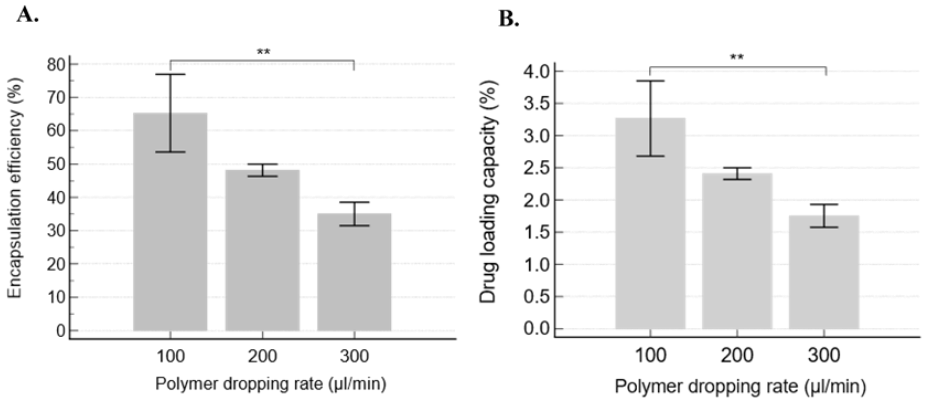

Figure 2: Effects of different polymer dropping rates on A) rutin encapsulation efficiency and B) drug loading capacity (n=3; mean±SD).

3.3 Visualization and particle size quantification of rutin-loaded PLA-PPEGMA particles

The morphology of PLA-PPEGMA particles was characterized using a scanning electron microscope (SEM) as shown in Figure 3A. The rutin-encapsulated particles exhibit spherical shapes with diameters ranged between 0.8 to 5.5 µm (Figure 3B) and mean particle size of 1.90 ± 0.71 µm. Particle size was one of the crucial factors for *in vivo* circulation, internalization by the cells, and the uptake pathway (Chen et al., 2003). There are multiple pieces of research indicated that the particles with the size of 50 nm are optimal for effective internalization and a higher rate of cellular uptake (Geiser et al., 2005; Zhu et al., 2013). Furthermore, particles in the size range between 30 – 50 nm can effectively internalize by receptor-mediated endocytosis (Wang et al., 2010). So, in future works, the reduction of particle size is required. To achieve the plan, we can get rid of large particle and particle agglomeration using various separation techniques such as filtration or centrifugation. Moreover, higher stirring speed during the encapsulation process may further reduce the particle size (Shi et al., 2012).

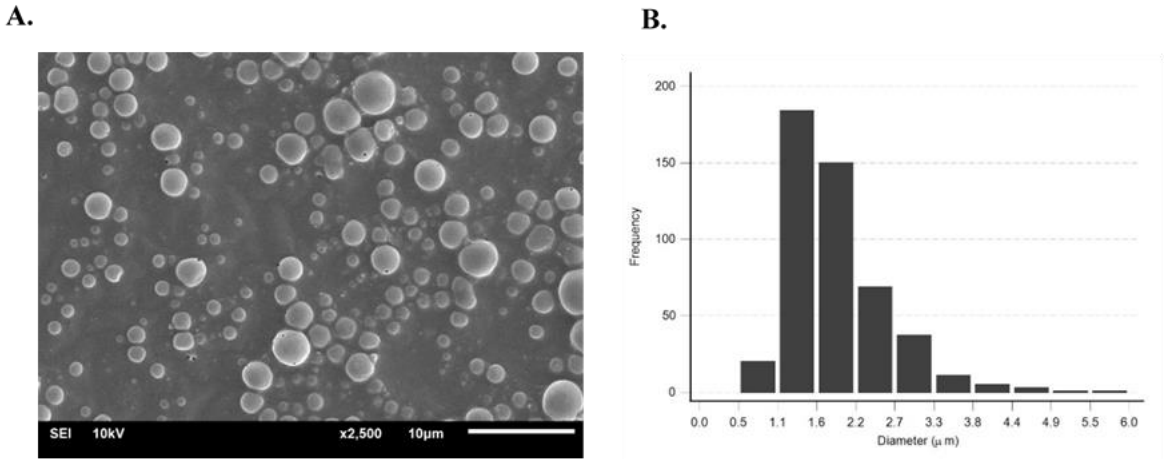

Figure 3: SEM image of A) Rutin-encapsulated PLA-PPEGMA particles and B) histogram of particle size distribution.

3.4 Determination of *in vitro* rutin release profile

The drug release behavior of free rutin and rutin-encapsulated particles were observed at different periods as shown in Figure 4. A rapid release profile was observed on free rutin. After approximately 45 min all the encapsulated rutin was released. On the other hand, as for rutin-encapsulated particles, the slower release profile was observed. The initial release during the first 45 min was 41.98 ± 17.15% which is more than 2 times slower than the release of free rutin. The release was continuously increased and reached 87.82 ± 0,95% in 4 hr.

The slower release of the rutin-encapsulated particles may be due to the PLA-PPEGMA property that sustains the encapsulated drug inside. These results indicated that the use of PLA-PPEGMA as a rutin encapsulated substance has the potential to prevent degradation and sustain the release of the drug. However, compared to the work of Saha and Mishra that encapsulated rutin using antisolvent precipitation technique, the burst and sustain release period of our particles is quite short (Saha & Mishra, 2020). Noted that the drug loading capacity is also one of the significant factors that affect drug release. Higher drug content would result in a low matrix polymer density, therefore, reducing the diffusional barrier.

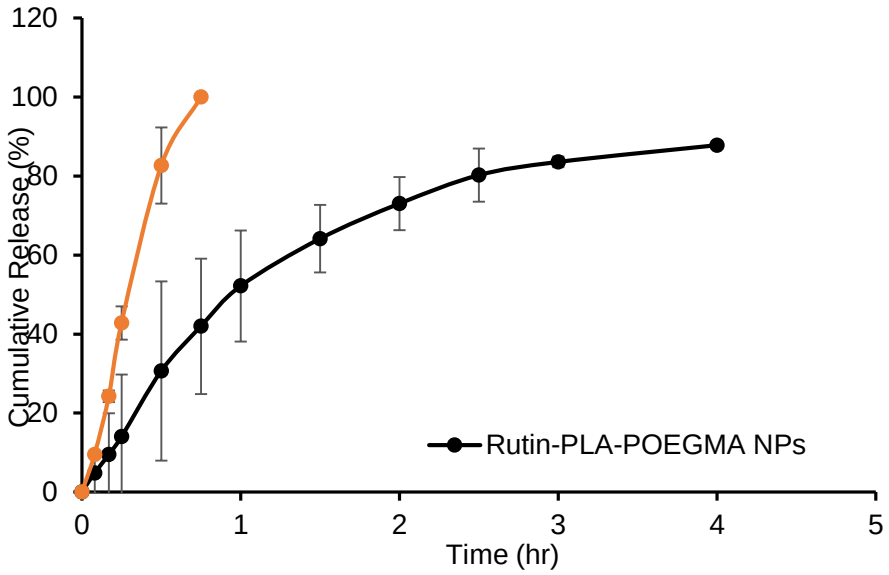

Figure 4: Cumulative drug release of free and particle-encapsulated rutin (n=3; mean±SD)

The kinetic release of rutin from PLA-PPEGMA particles was fitted to different mathematical models including zero order, first order, second order, Korsmeyer-Peppas, Weibull, and Hickson-Crowell. According to the results from KinetDS software, as shown in Table 3, the most appropriate mathematical model for rutin in PLA-PPEGMA release behavior was the Weibull kinetic model with the R^2 of 0.990 and shape parameter (b) of 1.18. According to Papadopoulou et al., when b is more than 1, the Weibull function indicates a complex release mechanism. The release rate is governed by the dissolution of PLA-PPEGMA combined with other release mechanisms (Papadopoulou et al., 2006).

Table 3: Coefficient of determination (R^2) for each model.

Encapsulation	Zero order	First order	Second order	Korsmeyer-Peppas	Weibull	Hickson- Crowell
Rutin-encapsulated PLA-PPEGMA particles	0.8648	0.1657	0.1003	0.9957	0.9990	0.6148

4. Conclusion

A solvent switch method could be used to efficiently encapsulated rutin by self-assembled PLA-PPEGMA. By optimizing the encapsulation protocols such as changing the drug/polymer ratio, the water volume used and the polymer dropping rates, better encapsulation efficiency and drug loading capacity can be achieved. These protocols are promising techniques for rutin encapsulation as well as the preparation of drug-encapsulated particles for drug delivery which could be applied for further biomedical applications. In our cases, the optimal protocol with optimal encapsulation efficiency was 0.5 mg rutin encapsulated by 10 mg PLA-PPEGMA under 5 mL water volume at 300 µl/min polymer dropping rate. The average particle size obtained was 1.90 ± 0.71 µm. However, the encapsulation efficiency and drug loading capacity can be

improved by decreasing the polymer dropping rates. Moreover, the encapsulation of rutin in self-assembled PLA-PPEGMA particles can prolong the release to more than 4 hr while free rutin can sustain the release for only 45 min. The release behavior conformed to the complex release mechanism of the Weibull kinetic model.

Acknowledgment

The authors thank Phoomintara Longsomboon for his help regarding chemical structure. This work was supported by KMUTT research fund.

References

Avsar, S. Y., Kyropoulou, M., Leone, S. Di, Schoenenberger, C. A., Meier, W. P., & Palivan, C. G. (2019). Biomolecules turn self-assembling amphiphilic block co-polymer platforms into biomimetic interfaces. *Frontiers in Chemistry*, *7*(JAN), 645. https://doi.org/10.3389/fchem.2018.00645

Cabral, H., Miyata, K., Osada, K., & Kataoka, K. (2018). Block Copolymer Micelles in Nanomedicine Applications. *Chemical Reviews*, *118*(14), 6844–6892. https://doi.org/10.1021/acs.chemrev.8b00199

Casalini, T., Rossi, F., Castrovinci, A., & Perale, G. (2019). A Perspective on Polylactic Acid-Based Polymers Use for Nanoparticles Synthesis and Applications. In *Frontiers in Bioengineering and Biotechnology* (Vol. 7). https://doi.org/10.3389/fbioe.2019.00259

Chen, W., Luo, W., Wang, S., & Bei, J. (2003). Synthesis and properties of poly(lactide)-poly(ethylene glycol) multiblock copolymers by coupling triblock copolymers. *Polymers for Advanced Technologies*, *14*(3–5), 245–253. https://doi.org/10.1002/pat.301

Fund, S., SAHNI, P., Shere, P. D., & Shere, D. (2018). Microencapsulation optimization and storage stability of curcumin in maltodextrin and gelatin. *Journal of Hill Agriculture*, *9*(4), 447–451.

Ganeshpurkar, A., & Saluja, A. K. (2017). The Pharmacological Potential of Rutin. *Saudi Pharmaceutical Journal*, *Feb;25*(2), 149–164. https://doi.org/10.1016/j.jsps.2016.04.025

Geiser, M., Rothen-Rutishauser, B., Kapp, N., Schürch, S., Kreyling, W., Schulz, H., Semmler, M., Im Hof, V., Heyder, J., & Gehr, P. (2005). Ultrafine particles cross cellular membranes by nonphagocytic mechanisms in lungs and in cultured cells. *Environmental Health Perspectives*, *113*(11), 1555–1560. https://doi.org/10.1289/ehp.8006

Joh, D. Y., Zimmers, Z., Avlani, M., Heggestad, J. T., Aydin, H. B., Ganson, N., Kumar, S., Fontes, C. M., Achar, R. K., Hershfield, M. S., Hucknall, A. M., & Chilkoti, A. (2019). Architectural Modification of Conformal PEG-Bottlebrush Coatings Minimizes Anti-PEG Antigenicity While Preserving Stealth Properties. *Advanced Healthcare Materials*, *8*(8), e1801177. https://doi.org/10.1002/adhm.201801177

Kianersi, F., Abdollahi, M. R., Mirzaie-asl, A., Dastan, D., & Rasheed, F. (2020). Identification and tissue-specific expression of rutin biosynthetic pathway genes in Capparis spinosa elicited with salicylic acid and methyl jasmonate. *Scientific Reports*, *10*(1), 8884.

https://doi.org/10.1038/s41598-020-65815-2

Kizilbey, K. (2019). Optimization of Rutin-Loaded PLGA Nanoparticles Synthesized by Single-Emulsion Solvent Evaporation Method. *ACS Omega*, *4*(1), 555–562. https://doi.org/10.1021/acsomega.8b02767

Martínez Rivas, C. J., Tarhini, M., Badri, W., Miladi, K., Greige-Gerges, H., Nazari, Q. A., Galindo Rodríguez, S. A., Román, R. Á., Fessi, H., & Elaissari, A. (2017). Nanoprecipitation process: From encapsulation to drug delivery. In *International Journal of Pharmaceutics* (Vol. 532, Issue 1, pp. 66–81). Elsevier B.V. https://doi.org/10.1016/j.ijpharm.2017.08.064

Motlekar, N. (2009). Optimization of experimental parameters for the production of LMWH-loaded polymeric microspheres. *Drug Design, Development and Therapy*, *2*(1), 39–48. /pmc/articles/PMC2761187/

Papadopoulou, V., Kosmidis, K., Vlachou, M., & Macheras, P. (2006). On the use of the Weibull function for the discernment of drug release mechanisms. *International Journal of Pharmaceutics*, *309*(1–2), 44–50. https://doi.org/10.1016/j.ijpharm.2005.10.044

Saha, S., & Mishra, A. (2020). A facile preparation of rutin nanoparticles and its effects on controlled growth and morphology of calcium oxalate crystals. *Journal of Crystal Growth*, *540*, 125635. https://doi.org/10.1016/j.jcrysgro.2020.125635

Shi, Y., Huang, W., Liang, R., Sun, K., Zhang, F., Liu, W., & Li, Y. (2012). Improvement of in vivo efficacy of recombinant human erythropoietin by encapsulation in PEG-PLA micelle. *International Journal of Nanomedicine*, *8*, 1–11. https://doi.org/10.2147/IJN.S38648

Su, K.-Y., Yu, C. Y., Chen, Y.-W., Huang, Y.-T., Chen, C.-T., Wu, H.-F., & Chen, Y.-L. S. (2014). Rutin, a Flavonoid and Principal Component of *Saussurea Involucrata*, Attenuates Physical Fatigue in a Forced Swimming Mouse Model. *International Journal of Medical Sciences*, *11*(5), 528–537. https://doi.org/10.7150/ijms.8220

Themistou, E., Battaglia, G., & Armes, S. P. (2014). Facile synthesis of thiol-functionalized amphiphilic polylactide- methacrylic diblock copolymers. *Polymer Chemistry*, *5*(4), 1405–1417. https://doi.org/10.1039/c3py01446k

Trucillo, P. (2021). Drug carriers: Classification, administration, release profiles, and industrial approach. *Processes*, *9*(3), 470. https://doi.org/10.3390/pr9030470

Wang, S. H., Lee, C. W., Chiou, A., & Wei, P. K. (2010). Size-dependent endocytosis of gold nanoparticles studied by three-dimensional mapping of plasmonic scattering images. *Journal of Nanobiotechnology*, *8*(1), 1–13. https://doi.org/10.1186/1477-3155-8-33

Xu, J., Chen, Y., Jiang, X., Gui, Z., & Zhang, L. (2019). Development of hydrophilic drug encapsulation and controlled release using a modified nanoprecipitation method. *Processes*, *7*(6), 331. https://doi.org/10.3390/pr7060331

Zhu, M., Nie, G., Meng, H., Xia, T., Nel, A., & Zhao, Y. (2013). Physicochemical properties determine nanomaterial cellular uptake, transport, and fate. *Accounts of Chemical Research*, *46*(3), 622–631. https://doi.org/10.1021/ar300031y